Journal of Alloys and Compounds 479 (2009) 674–677

Contents lists available at ScienceDirect

Journal of Alloys and Compounds

journal homepage: www.elsevier.com/locate/jallcom

Optoelectronic characteristics of UV photodetector based on ZnO nanowire thin films

K.J. Chen [a], F.Y. Hung [b,*], S.J. Chang [a], S.J. Young [a]

[a] Institute of Microelectronics & Department of Electrical Engineering, Center for Micro/Nano Science and Technology, National Cheng Kung University, Tainan 701, Taiwan
[b] Institute of Nanotechnology and Microsystems Engineering, Center for Micro/Nano Science and Technology, National Cheng Kung University, No. 1, Ta-Hsueh Road, Tainan 701, Taiwan

ARTICLE INFO

Article history:
Received 19 October 2008
Accepted 12 January 2009
Available online 23 January 2009

Keywords:
ZnO
Thin film
Nanowires

ABSTRACT

The ZnO thin films were prepared on the quartz substrate by the sol–gel method and the UV photodetector was constructed on the ZnO thin films, with a circular spiral structure in contact 30 nm IrO_2 electrodes. The ZnO thin films were crystallized at various temperatures (600–700 °C) for 1 h in a pure oxygen atmosphere, then were analyzed by X-ray diffraction (XRD) and scanning electron microscopy (SEM) to investigate the crystallized thin film structures. From photoluminescence (PL) and *I–V* measurements, the 650 °C thin film not only possessed better crystallization but also had nanowire structures that revealed excellent potential as a UV photodetector.

1. Introduction

Photodetectors operating in the UV region are important devices that can be used in many commercial and military applications, such as ozone layer monitoring, flame detection and missile warning systems [1,2], etc. In recent years, UV photodetectors have been fabricated on wide direct bandgap materials. Notably, ZnO possesses a wide direct band-gap energy of 3.37 eV and a larger exciton-binding energy of 60 meV [3], that have been used by several deposition techniques, such as RF magnetron sputtering, molecular beam epitaxy (MBE), metal organic chemical vapor deposition (MOCVD), pulsed laser deposition (PLD) and the sol–gel process [4–8]. Among these methods, the sol–gel method enjoys the advantages of being able to prepare large area ZnO thin films at low cost and easy technology [9]. Therefore, several investigations have prepared UV photodetectors using sol–gel synthesized ZnO thin films [10,11]. However, how the crystallization of sol–gel ZnO thin film affects the optoelectronic characteristics has still not been investigated. In addition, almost all the photodetector devices used interdigital (IDT) circular structures as contact electrodes [12,13], and the effect of the spiral configuration is worthy of further investigation.

To improve the quality of the photodetector, the metal electrodes need a higher work function and a higher thermal stability [14,15]. But, many electrodes with high work function are not stable at higher temperatures. Iridium (Ir) metal has some advantages in terms of thermal (1000 °C) and chemical stability [16,17]. In addition, iridium oxide (IrO_2) also has some advantages, such as high work function (>5 eV), excellent thermal stability and high transmittance [18,19], and so can be used in the electrodes of photodetectors [20,21].

For these reasons, this study used sol–gel derived ZnO thin films with an 30 nm Ir electrode to fabricate the UV photodetector, on order not only to understand the effect of different crystallizations, but also investigate the contribution of the spiral electrode configuration.

2. Experimental procedure

The ZnO thin films were deposited on the quartz substrate using the sol–gel method. To prepare the aqueous solution of ZnO, 2 M zinc acetate dehydrate ($Zn(CH_3COO)_2{\cdot}2H_2O$) was synthesized with a diethanolamine (DEA) in hydranal methanol (dry ≤ 0.01% water), and the molar ratio of DEA to zinc acetate was 1 [22]. The aqueous solution was stirred at 140 °C for 3 h to form a homogeneous and transparent solution. The spin coating method with a rotation rate of 3000 rpm was used to coat all substrates. After that, the film samples were dried at 200 °C for 10 min to evaporate the solvent and remove organic residuals, and then were naturally cooled to room temperature (10 times consecutively). Finally, the film samples were subjected to different crystallizing temperatures (600 °C, 650 °C and 700 °C) for 1 h under O_2 atmosphere with a flow rate of 50 sccm. The thickness of the ZnO thin film was approximately 250 nm which was measured by a dual-beam focused ion beam (FIB) (not given here).

UV photodetectors were fabricated and based on circular spiral metal-semiconductor-metal (MSM) structures. Iridium (Ir) film of thickness 30 nm was patterned onto the surface of sol–gel derived ZnO film by electron beam evaporation to serve as the metal contacts. The width and space of the contact electrodes were 300 μm, and the active area of the UV photodetector was 6000 μm × 4000 μm. Finally, the Ir electrode contact was annealed at 500 °C for 10 min under an O_2

* Corresponding author. Tel.: +886 6 2757575x31395; fax: +886 6 2745885.
E-mail address: fyhung@mail.mse.ncku.edu.tw (F.Y. Hung).

0925-8388/$ – see front matter © 2009 Elsevier B.V. All rights reserved.
doi:10.1016/j.jallcom.2009.01.026

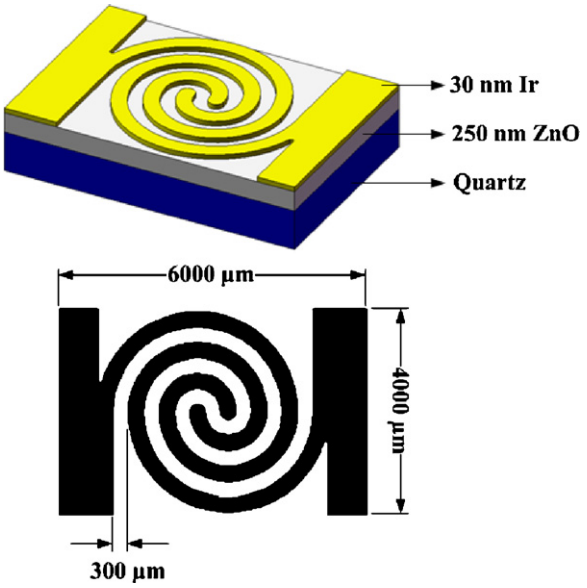

Fig. 1. The schematic structure of ZnO MSM photodetector.

atmosphere with a flow rate of 50 sccm. The schematic structure of the MSM UV photodetectors is shown in Fig. 1.

In addition, the crystalline structure was analyzed by thin-film X-ray diffraction (XRD), scanning electron microscopy (SEM) and a dual-beam focused ion beam (DB-FIB). The photoluminescence (PL) measurement was used to analyze the optical properties of ZnO crystallization by 325 nm UV light from a He–Cd laser at room temperature. Also, the current–voltage (*I–V*) characteristics of the devices were measured by a HP 4145 semiconductor parameter analyzer in both the darkness and illumination. The top-illuminated spectral response was quantified using a 250 W xenon (Xe) arc lamp light source and calibrated for a monochromatic detection in the range of 300–450 nm.

3. Results and discussion

3.1. Structural characteristics

The XRD patterns of ZnO thin films with different crystallization temperatures (600 °C, 650 °C and 700 °C) are shown in Fig. 2. All the ZnO thin films corresponded to the wurzite-type ZnO structure and preferred an orientation of (0 0 2). With increasing the crystallization temperature from 600 °C to 650 °C, the intensity of the (0 0 2) diffraction peak increased, revealing that the crystallization of the ZnO thin film was improved by an adequate supply of thermal energy [22]. In general, the quality of the ZnO films was able

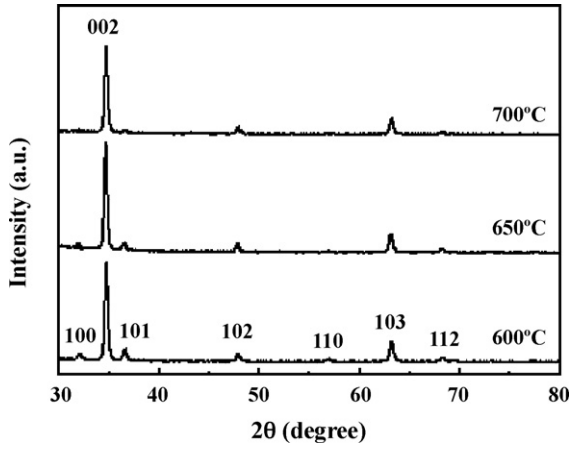

Fig. 2. XRD patterns of ZnO thin films with different crystallized temperature.

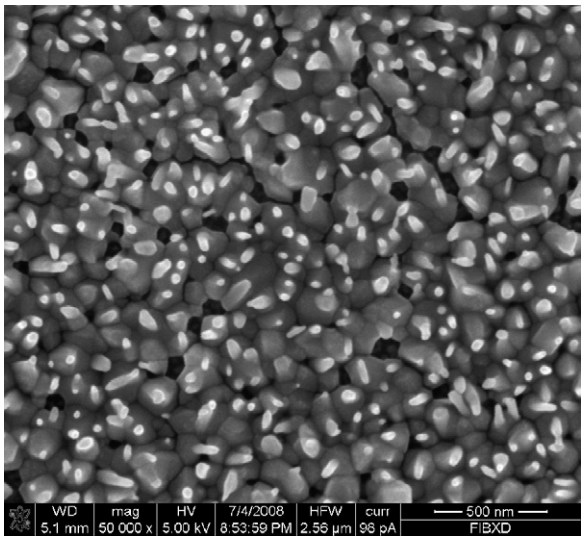

Fig. 3. The surface morphology of 650 °C ZnO film.

to be improved by increasing the annealing temperature [23–25]. However, the crystallization mechanism of the ZnO thin film began to deteriorate at 700 °C. The main reason is that variations in the grain boundary energy made some of the grains grow unusually and destroyed the crystallization of the ZnO thin film under higher crystallization temperatures.

For 650 °C ZnO film, the (0 0 2) diffraction peak at $2\theta = 34.7^\circ$ with a full-width half-maximum (FWHM) of 0.38° showed the excellent quality of the ZnO thin film. The surface morphology of the 650 °C ZnO thin film is shown in Fig. 3. The film shows a large amount of grain boundaries and a few micro-pore structures scattered on the surface. These micro-pore structures are certain to appear on the sol–gel synthesized ZnO thin films [25]. Notably, some nucleus-like structure was found on the grain surface (Fig. 3). When the surface image was rotated from 0° to 52° using FIB (from top view to side view), the nucleus-like structure could be identified as ZnO nanowires (Fig. 4). The length of the nanowires was approximately ~90 nm and grew disorderly on the film matrix. This result was that the residual zinc reacted with oxygen to form the ZnO nuclei. Increasing the duration of crystallization, the ZnO nuclei individually grew to form the ZnO nanowires. However, under higher

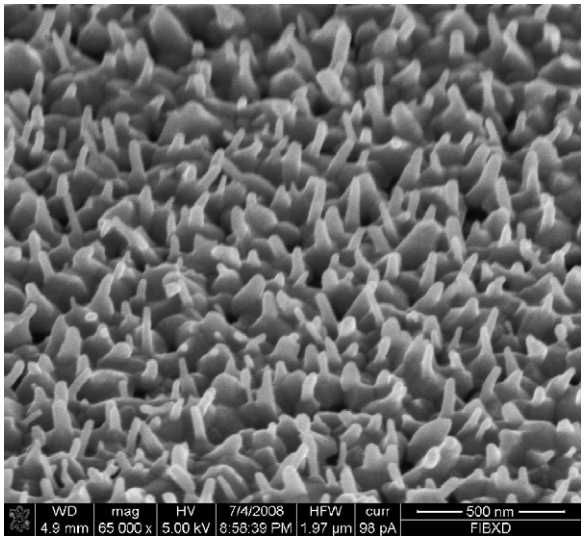

Fig. 4. Surface characteristic of 650 °C ZnO film with nanowires (using FIB).

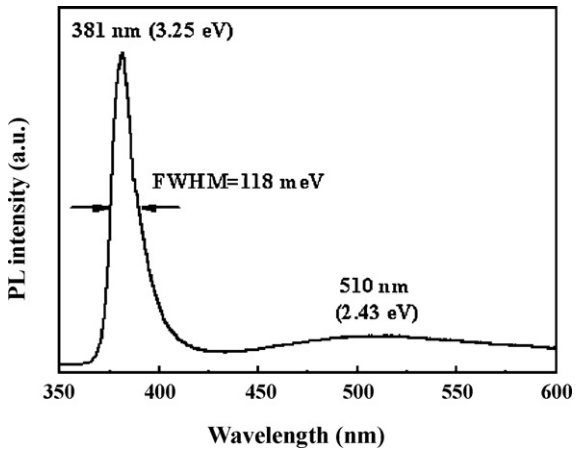

Fig. 5. PL spectrum of ZnO thin film at room temperature.

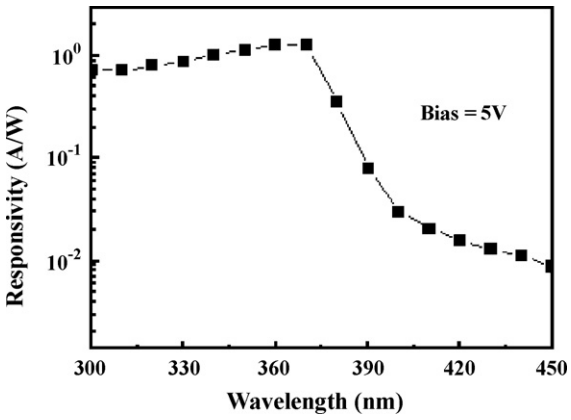

Fig. 7. The spectral response of the photocurrent measurement of ZnO MSM photodetector.

crystallization temperatures, the unusual growth of the grains not only restrained the growth of the ZnO nanowires, but also destroyed the crystallization. This is why the 650 °C ZnO thin film possessed the best crystallization mechanism.

3.2. Optical and electrical properties

The 650 °C films had excellent crystallized structures with nanowires. Photoluminescence (PL) was used to check its optical quality. Fig. 5 shows the PL spectrum (room temperature) of sol–gel derived ZnO thin film. In the spectrum, the ZnO thin film contains a strong UV emission band at 381 nm (3.25 eV) and a very weak green emission band at 510 nm (2.43 eV), which can be attributed to the recombination of free excitons [26] and oxygen vacancies in the ZnO lattice [27,28]. In addition, the full-width half-maximum of the UV emission band was 118 meV. This results indicate that the crystallization of the ZnO thin film was just as good as ZnO epitaxial film produced by radio frequency (RF) or plasma-assisted MBE [28].

The IrO_2/ZnO/IrO_2 MSM structure with a circular spiral configuration was used to evaluate the UV detector performance. The *I–V* characteristic of the ZnO photodetector was measured in darkness and under photoillumination in Fig. 6. Under a 5 V applied bias, it was found that the dark current was 5.11×10^{-7} A and the photocurrent was 4.32×10^{-9} A. In other words, the photocurrent was about two orders of magnitude larger than the dark current. Similar results have been obtained in relevant reports [12,29]. Notably, the photocurrent and dark current differed by less than one order of magnitude. It is clear that the electrical properties of the present thin film had been enhanced. In addition, Fig. 7 shows the spectral response of the photocurrent measurement on the MSM ZnO photodetector. For a light wavelength of 360 nm and 5 V applied bias, the response was 0.011 A/W and the cut-off occurred at 370 nm (Fig. 7). Although the cut-off was not sharp, the present structure had higher photocurrent value than two orders of magnitude from 370 nm to 420 nm. We can be confident that the sensitivity of the sol–gel derived ZnO thin film with nanowires in the UV region is good enough for applications as UV photodetector materials.

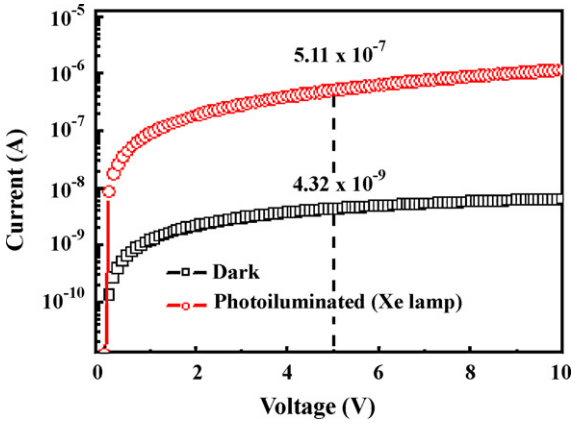

Fig. 6. *I–V* characteristics of ZnO photodetector measured in dark and under Xe illumination.

4. Conclusion

The 650 °C sol–gel derived ZnO thin film not only possessed a better crystallized mechanism, but also had nanowires on the film surface that were able to enhance the opto-electronic properties of the UV photodetector. For *I–V* measurement, the curve corresponded to the schottky metal-semiconductor contacts and the photo-generated current arrived at 5.11×10^{-7} A under a bias voltage of 5 V. In addition, the photocurrent was 2 orders of magnitude larger than the dark current, quite adequate for a UV photodetector.

Acknowledgements

The authors are grateful to National Cheng Kung University, the Center for Micro/Nano Science and Technology (NCKU Project of D97-2700) and NSC 97-2221-E-006-018/NSC 97-2622-E-006-009-CC3 for the financial support.

References

[1] P. Sandvik, K. Mi, F. Shahedipour, R. McClintock, A. Yasan, P. Kung, M. Razeghi, J. Cryst. Growth 231 (2001) 366–370.
[2] C. Varenne, L. Maezt, J. Brunet, K. Wierzbowska, A. Pauly, B. Lauron, Thin Solid Films 516 (2008) 2237–2243.
[3] M.H. Huang, Y. Wu, H. Feick, N. Tran, E. Weber, P. Yang, Adv. Mater. 13 (2001) 113–116.
[4] T. Matsuda, M. Furuta, T. Hiramatsu, C. Li, H. Furuta, T. Hirao, Appl. Surf. Sci. 310 (2008) 31–35.
[5] H.J. Lee, S.H. Lee, F. Yildiz, Y.H. Jeong, J. Magn. Magn. Mater. 310 (2007) 2089–2091.
[6] X. Li, B. Zhang, H. Zhu, X. Dong, X. Xia, Y. Cui, K. Huang, G. Du, Appl. Surf. Sci. 254 (2008) 2081–2084.
[7] P.K. Shin, Y. Aya, T. Ikegami, K. Ebihara, Thin Solid Films 516 (2008) 3767–3771.
[8] M. Dutta, S. Mridha, D. Basak, Appl. Surf. Sci. 254 (2008) 2743–2747.
[9] S. Hwangbo, Y.J. Lee, K.S. Hwang, Ceram. Int. 34 (2008) 1237–1239.
[10] D. Basak, G. Amin, B. Mallik, G.K. Paul, S.K. Sen, J. Cryst. Growth 256 (2003) 73–77.
[11] P.T. Hsieh, Y.C. Chen, K.S. Kao, C.C. Cheng, J. Eur. Ceram. Soc. 27 (2007) 3815–3818.
[12] Z.Q. Xu, H. Deng, J. Xie, Y. Li, X.T. Zu, Appl. Surf. Sci. 253 (2006) 476–479.
[13] S.J. Young, L.W. Ji, T.H. Fang, S.J. Chang, Y.K. Su, X.L. Du, Acta Mater. 55 (2007) 329–333.

[14] S.N. Mohammad, Z. Fan, A.E. Botchkarev, W. Kim, O. Aktas, A. Salvador, Electron. Lett. 32 (1996) 598–599.
[15] A.C. Schmitz, A.T. Ping, M.A. Khan, Q. Chen, J.W. Yang, I. Adesida, Electron. Lett. 32 (1996) 1832–1833.
[16] S.J. Young, L.W. Ji, S.J. Chang, Y.P. Chen, K.T. Lam, S.H. Liang, X.L. Du, Q.K. Xue, Y.S. Sun, IET Optoelectron. 1 (2007) 135–139.
[17] L.F. Voss, L. Stafford, B.P. Gila, S.J. Pearton, F. Ren, Appl. Surf. Sci. 254 (2008) 4134–4138.
[18] L.F. Mattheiss, Phys. Rev. B 13 (1976) 2433–2450.
[19] H.W. Kim, S.H. Shim, J.H. Myung, C. Lee, Vacuum 82 (2008) 1400–1403.
[20] J.K. Kim, H.W. Jang, C.M. Jeon, J.L. Lee, Appl. Phys. Lett. 81 (2002) 4655–4657.
[21] S.S. Thanawala, R.J. Baird, D.G. Georgiev, G.W. Auner, Appl. Surf. Sci. 254 (2008) 5164–5169.
[22] K.J. Chen, T.H. Fang, F.Y. Hung, L.W. Ji, S.J. Chang, S.J. Young, Y.J. Hsiao, Appl. Surf. Sci. 254 (2008) 5791–5795.
[23] S.B. Majumder, M. Jain, P.S. Dobal, R.S. Katiyar, Mater. Sci. Eng. B 103 (2003) 16–25.
[24] Q. Yu, H. Yang, W. Fu, L. Chang, J. Xu, C. Yu, R. Wei, K.D. Hongyang, M. Li, G. Zou, Thin Solid Films 515 (2007) 3840–3843.
[25] P.T. Hsieh, Y.C. Chen, K.S. Kao, M.S. Lee, C.C. Cheng, J. Eur. Ceram. Soc. 27 (2007) 3815–3818.
[26] W.D. Yu, X.M. Li, X.D. Gao, Appl. Phys. Lett. 84 (2004) 2660–2685.
[27] Y.C. Liu, Y.W. Chen, C.L. Shao, S.X. Lu, J. Sol–Gel Sci. Technol. 39 (2006) 57–62.
[28] S.J. Young, L.W. Ji, S.J. Chang, Y.K. Su, J. Cryst. Growth 29 (2006) 43–47.
[29] J.H. He, Y.H. Lin, M.E. McConney, V.V. Tsukruk, Z.L. Wang, G. Bao, J. Appl. Phys. 102 (2007) 084303.